

Caustic Crossing in the Gravitational Lens Q2237+0305

V. N. Shalyapin *

*Institute of Radio Astronomy, National Academy of Sciences of Ukraine,
Kharkov, Ukraine*

Received April 4, 2000; in final form, September 13, 2000

The monitoring of the gravitational lens Q2237+0305 carried out by the OGLE group during 1997–1999 is analyzed. The significant light amplifications in the C and A quasar components with maxima in mid- and late 1999, respectively, are interpreted as the crossing of microlens caustics by the source. A constraint on the emitting-region size $R \leq 10^{15}$ cm has been obtained from the light-curve shape by assuming a power-law quasar brightness distribution $(r^2 + R^2)^{-p}$. To estimate the exponent $p \sim 1.2$ requires refining the standard model for the quasar continuum formation in an optically thick accretion disk with $p = 1.5$.

Key words: quasars, gravitational lenses, accretion disks

1 INTRODUCTION

Quasar variability under the effect of microlenses depends both on parameters of the mass distribution for compact bodies and on the appearance of the emitting region. For instance, the larger is the quasar, the smaller are the amplitudes of light variations in its images. Thus, it becomes possible to formulate the inverse problem of determining the sizes and structure of quasars from their observed light curves. The main difficulty in solving this problem is that the distribution of the amplification produced by microlenses is not known in advance and exhibits a fairly complex pattern with many randomly located caustic lines (see, e.g., Zakharov 1997 and Zakharov and Sazhin 1998). In general, the specific

*E-mail address for contacts: vshal@ira.kharkov.ua

form of this distribution is not known and can be analyzed only statistically. Exceptions are only those portions of the light curve that correspond to caustic crossing by the quasar. The amplification of a point source during caustic crossing obeys a simple law: it remains approximately constant as the caustic is approached, then abruptly increases to infinity at the caustic itself, and subsequently falls off as $x^{-1/2}$ with increasing distance x from the caustic (Chang and Refsdal 1984; Blandford and Narayan 1986).

Microlenses must show up most clearly in the multiple quasar images produced by the gravitational effect of galaxy macrolenses. First, the microlensing probability is rather high in such situations. Second, intrinsic quasar variability can, in principle, be separated from microlensing variability. Of all the gravitationally lensed quasars, Q2237+0305 ($z_s = 1.675$) is undoubtedly the most promising object for microlensing analysis. Because the unique proximity of a lensing galaxy ($z_l = 0.039$), microlensing variability in this object must take place faster than in other objects by an order of magnitude and with a large amplitude.

The quasar Q2237+0305 has been monitored virtually since its discovery, and it actually proved to be the first object in which microlensing variability was detected (Irwin et al. 1989; Corrigan et al. 1991). The observations by Østensen et al. (1996) showed that virtually all four quasar images were more or less variable.

The regularity and quality of the Q2237+0305 monitoring have improved markedly when the OGLE group joined it in the last four years (Wozniak et al. 2000) (see Fig. 1). Measurements are made in the V band approximately once a week during the observing season from May through December. The latest observations (<http://www.astro.princeton.edu/~ogle/ogle2/huchra.html>) show that image C passed its intensity peak in mid-1999, while image A peaked in late 1999. Interpreting the light-curve maxima as resulting from caustic crossing allows the size and structure of the quasar emitting region in the object under study to be determined.

2 AMPLIFICATION OF AN EXTENDED SOURCE IN THE CAUSTIC REGION

When a source crosses a caustic line, an additional pair of images appears (or disappears). The total intensity of this pair depends on the distance to the caustic as $x^{-1/2}$. Therefore, the intensity of a point source in the caustic region can be represented as (Schneider and Weiss 1987)

$$I_p(x) = I_0 + \theta(x)a_0x^{-1/2}. \quad (1)$$

Here, I_0 is the intensity of all the remaining microimages except the additional pair, $\theta(x)$ is the Heaviside unit function, and a_0 is the caustic strength. The amplification of an extended source with a brightness distribution $P(\mathbf{r})$ can be calculated by ordinary summation over the set of infinitely small sources with

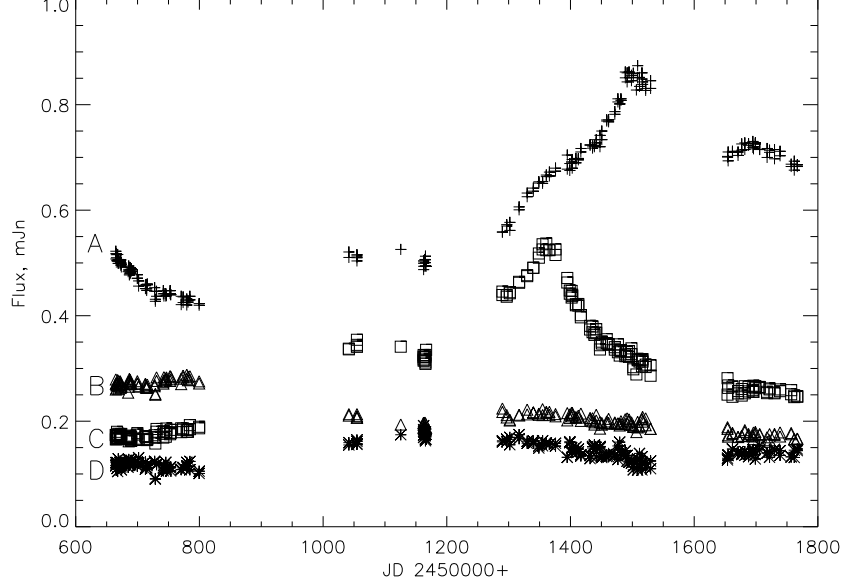


Figure 1: V light variations of the four images of the quasar Q2237+0305 during 1997–2000 as observed by the OGLE group

individual amplification factors:

$$I = \left[\int d\mathbf{r} P(\mathbf{r}) I_p(\mathbf{r}) \right] / \left[\int d\mathbf{r} P(\mathbf{r}) \right]. \quad (2)$$

To describe the brightness distribution in the source, we use a power-law model

$$P(r) = \left(1 + \frac{r^2}{R^2}\right)^{-p} \quad (p > 0), \quad (3)$$

which is determined by the source radius R and by the rate of brightness decline p .

Let the source center be at a distance D from the caustic line. In the normalized coordinates $\xi = x/R$ and $\eta = y/R$ and using normalized distance $d = D/R$, we obtain

$$I = I_0 + a_0 R^{-1/2} J(d), \quad (4)$$

where the function $J(d)$ is

$$J(d) = \left[\int_{-\infty}^{+\infty} d\eta \int_0^{+\infty} d\xi P(\xi, \eta) \xi^{-1/2} \right] / \left[\int_{-\infty}^{+\infty} d\eta \int_{-\infty}^{+\infty} d\xi P(\xi, \eta) \right] \quad (5)$$

or, taking into account the symmetry in η and the total intensity

$$\int P(r) d\mathbf{r} = \frac{\pi R^2}{p-1}, \quad (6)$$

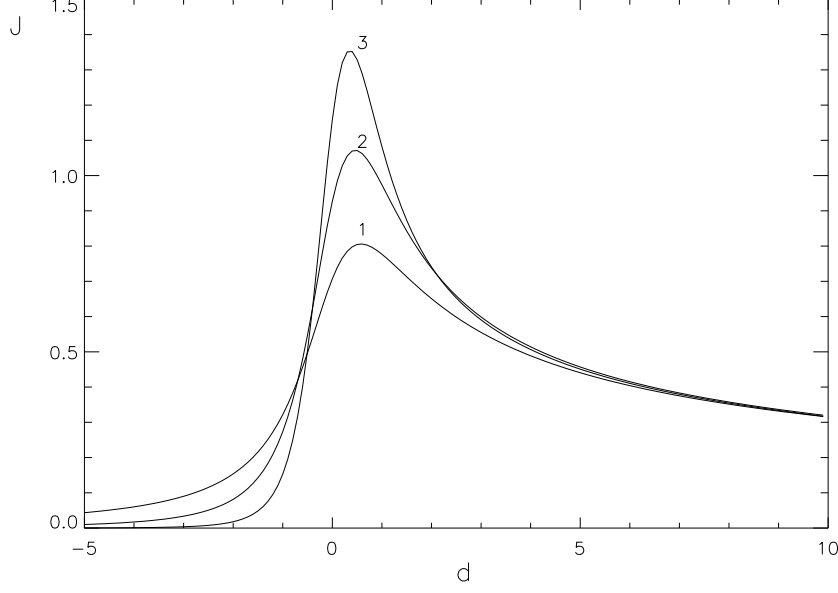


Figure 2: Function $J(d)$ for several exponents p : curve 1, 2, and 3 for $p = 1.5$, 2.0, and 3.0, respectively

we obtain:

$$J(d) = 2 \frac{p-1}{\pi} \int_0^\infty d\xi \int_0^\infty d\eta \xi^{-\frac{1}{2}} [1 + (\xi - d)^2 + \eta^2]^{-p}. \quad (7)$$

Taking the internal integral over η yields

$$J(d) = \frac{p-1}{\pi} \int_0^\infty d\xi B\left(\frac{1}{2}, p - \frac{1}{2}\right) \xi^{-1/2} [\xi^2 - 2\xi d + d^2 + 1]^{\frac{1}{2}-p}, \quad (8)$$

where B is the beta function. The subsequent integration over ξ yields

$$J(d) = \frac{\Gamma(p - \frac{1}{2})\Gamma(2p - \frac{3}{2})}{\Gamma(p-1)\Gamma(2p-1)} (1 + d^2)^{\frac{3}{4}-p} {}_2F_1\left(\frac{1}{2}, 2p - \frac{3}{2}; p; \frac{1}{2} \left(1 + \frac{d}{\sqrt{1+d^2}}\right)\right). \quad (9)$$

Here, Γ and ${}_2F_1(a, b; c; z)$ are the gamma function and the Gauss hypergeometric function, respectively. Figure 2 shows the function $J(d)$ for several values of p . We clearly see from the figure that the sharpness of the jump in amplitude increases with increasing source brightness concentration toward the center during caustic crossing, tending to an infinite point-source limit for very large p .

For some particular p values, for example, for $p = 3/2, 2$ and 3 , the hypergeometric function can be expressed as a combination of elementary and other

special functions. Thus, we have for $p = 3/2$

$$J(d)|_{p=3/2} = \left[2(1 + d^2)((1 + d^2)^{1/2} - d) \right]^{-1/2}. \quad (10)$$

3 VARIABILITY ANALYSIS

We see from Fig. 1 that the intensities of all four quasar images have varied during the last four years. The largest variations were observed in image C, which passed its maximum in mid-1999, and in image A, which reached its maximum in late 1999. The approach to interpreting the variability of these two images is the same. Let us assume that, in both cases, the source crosses the caustic; the brightness distribution must follow the law (4). The general form of the curve depends on five parameters:

1. Contribution I_0 from the remaining microimages, which is assumed to be approximately constant;
2. Caustic strength a_0 ;
3. The time it takes for the source to cross its radius Δt of the source, which is proportional to the source size R ;
4. The time t_0 of caustic crossing by the source center;
5. Exponent p in the brightness distribution (3).

Estimating the five parameters reduces to minimizing the sum of the squared differences between model and observed light curves

$$\chi^2 = \sum_{i=1}^N \frac{1}{\sigma_i^2} [I_{model}(I_0, a_0, \Delta t, t_0, p) - I_{obs}]^2. \quad (11)$$

The summation is performed over all N points of observations with weights that are inversely proportional to the squares of the observational errors σ_i . The best set of parameters is sought by the Marquardt method (see, e.g., Chapter 15.5 in the book by Press et al. 1992).

3.1 Image A

The model parameters estimated from the light curve of image A with 182 data points during the entire observing period 1997-1999 are given in the Table 1. The combination $a_0/\Delta t$ is more convenient to calculate than the caustic strength a_0 . The listed formal accuracies of the parameter estimates should be considered only as their lower limits.

Figure 3 shows the model light curve together with measured values. The 1997 observations are poorly fitted by a single curve, implying that approaching the caustic did not show up in the first year. Such a behavior is characteristic

Image	I_0	$a_0/\Delta t$	Δt	t_0	p
A 1997-1999	0.44 ± 0.01	0.73 ± 0.07	91 ± 4	1462 ± 1	1.24 ± 0.03
C 1998-1998	0.22 ± 0.01	0.95 ± 0.15	-29 ± 2	1390 ± 1	1.10 ± 0.02

Table 1: Best-fit model parameters

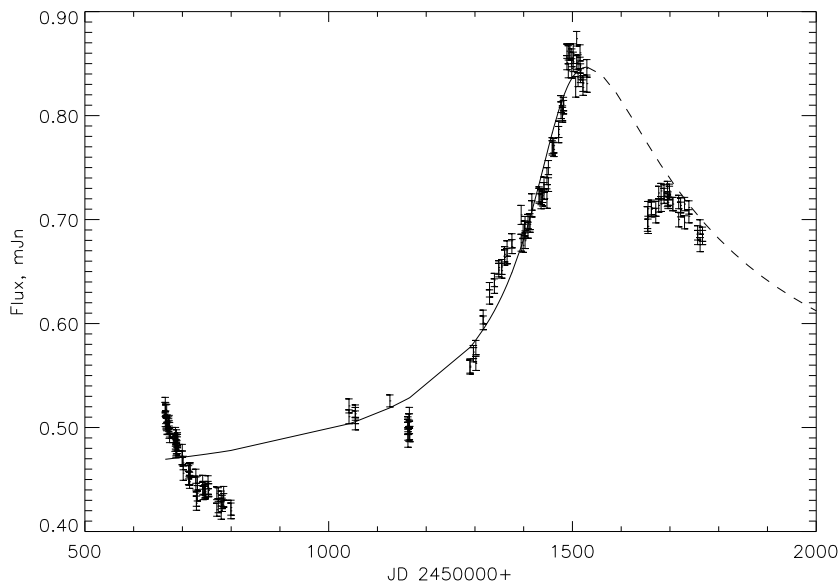


Figure 3: Variability of image A during 1997–2000. Observational data, model, and forecast

of numerical microlensing models for Q2237+0305, in which one amplification event is often superimposed on another to form complex light curves. Excluding the 1997 data from our analysis, while significantly improving the total χ^2 residual, affects the parameter estimates only slightly.

When the caustic is crossed in image A, an additional pair of images emerges. A characteristic feature of this direction of motion is a steep rise in light amplification followed by a gentler decline. The dashed line in Fig. 3 represents the expected behavior of image A in the immediate future. We assume that the brightness will continue to decline and (if no additional causes of amplification arise) will reach the original 1997 level in two to three years. The latest observations for 2000 are added for comparison.

3.2 Image C

Attempts to fit the light curve of image C over the entire observed period have failed. At the same time, excluding 80 data points for 1997 from our analysis results in quite reasonable estimates, which are given in the table and shown in

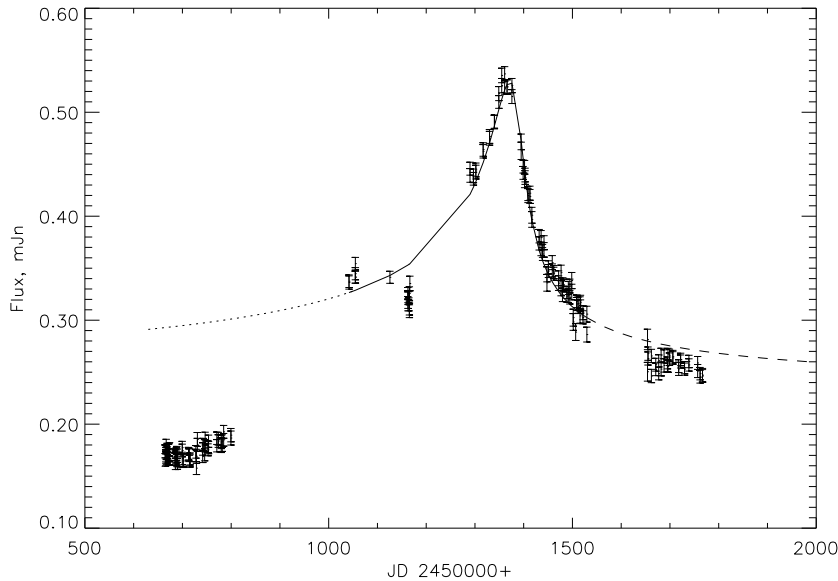


Figure 4: Light curve of image C during 1997–2000. Observations, model (dotted line), and forecast

Fig. 4. Interestingly, the best solution corresponds to caustic crossing in the negative direction, with the pair of images disappearing. The local minimum of χ^2 corresponding to the motion in the positive direction is several times greater than the absolute minimum reached during the motion in the negative direction.

The inability to fit the entire observed period by a single curve becomes more understandable in light of the recent results by Wyithe et al. 2000. These authors argue that the intensity variations in image C have been composite in pattern during the last four years, and, what is quite possible, another caustic crossing was overlooked during the observing seasons in 1997 and 1998.

The dotted and dashed lines indicate the best extrapolation computed in the model with single caustic crossing in 1997 and our forecast until the end of 2000, respectively. No appreciable intensity variations in image C are expected in the immediate future.

4 THE SIZE AND STRUCTURE OF THE QUASAR EMITTING REGION

For the quasar radius estimates Δt in time units to be transformed to linear sizes R , we must know the apparent quasar velocity; only the velocity component v_{\perp} is perpendicular to the caustic line is important. Of course, the exact velocity is unknown. Nevertheless, a statistical analysis of the time derivatives of brightness variations by Wyithe et al. 1999 yielded an upper limit of $v < 500$

km/s . The perpendicular velocity component can only be lower than this value. The most probable value of v_{\perp} was found to be $300 km/s$. Given the angular distances from the observer to the quasar D_{os} and to the lens D_{ol} in the model of a flat Universe with $H_0 = 60 km/s Mpc^{-1}$, the most probable source radius is estimated to be

$$R = v_{\perp} \Delta t \frac{D_{os}}{D_{ol}} \sim 2.0 \cdot 10^{13} \left(\frac{v_{\perp}}{300 km/s} \right) \left(\frac{\Delta t}{1 day} \right) cm. \quad (12)$$

Using the crossing time $\Delta t_A = 90 days$ for image A gives the most probable quasar radius $R = 1.8 \cdot 10^{15} cm$, while substituting the crossing time for image C, $\Delta t_C = 30 days$, reduces this estimate to $R = 6 \cdot 10^{14} cm$. At the same time, the velocity constraint $v < 500 km/s$ together with the crossing time Δt_C give an upper limit on the source radius, $R \leq 10^{15} cm$.

Another parameter that characterizes the mass distribution is the exponent p . It follows from the table that its computed value lies between 1.1 and 1.25. It is interesting to note that different models for the quasar structure can lead to different dependences of the emissivity on distance from the center. For instance, a power-law dependence with $p \leq 0.5$ follows from the model of an optically thin accretion disk (Manmoto et al. 1997). At the same time, the standard model of an optically thick accretion disk yields an r^{-3} dependence (Shakura and Sunyaev 1973), which changes to $(r^2 + R^2)^{-3/2}$ for a finite radius. Our estimate $p \sim 1.2$ favors the standard model, but more complex accretion-disk models should be analyzed to achieve better agreement.

5 DISCUSSION

Let us consider the legitimacy of some assumptions made here. The main assumption is associated with the hypothesis of caustic crossing. Numerical calculations show that there are two effects capable of causing a significant increase in amplification. Apart from fold-caustic crossing, the source can also pass near the caustic cusp. However, events of the second type for the images of Q2237+0305 are several times less probable than those of the first type (Wambsganss et al. 1992; Lewis and Irwin 1996) and, in general, are more symmetric. These two properties can serve as a statistical justification for using the hypothesis of caustic crossing.

A power-law model with a finite core radius is used to calculate the quasar size and structure. Three models of a caustic-crossing source are encountered in the literature: a homogeneous disk, a Gaussian source (Schneider and Weiss 1987), and a $(1 - r^2/R^2)^{1/2}$ distribution (Schneider and Wagoner 1987). All of them are completely determined by their radii. The $(1 + r^2/R^2)^{-p}$ model differs radically in that it is a two-parameter model. Estimating the rate of brightness decline p allows us to choose between different models for the quasar structure.

Allowance for the spatial orientation of the emitting region appreciably complicates the analysis. Two additional parameters associated with the orientation-angle components of the initial circular source appear. The first and second

parameters determine, respectively, the apparent-ellipse eccentricity and the angle of motion with respect to the perpendicular to the caustic (in this case, allowance for the direction of motion does not reduce to a simple substitution of the transverse velocity). Besides, accretion-disk rotation can cause an additional asymmetry of the emitting region in the spectral range considered due to the Doppler effect.

In view of many influencing factors, the possibility of reconstructing, at least in principle, the one-dimensional quasar profile (along the x -axis) as the solution of an integral equation (Grieger et al. 1991; Mineshige and Yonehara 1999; Agol and Krolik 1999) seems of great interest. However, this is a separate, independent problem, which is yet to be applied to an actual monitoring.

The simple amplification behavior $\sim x^{-1/2}$ for a point source located in the caustic region is possible only when several conditions are satisfied. The radius of caustic curvature must be considerably larger than the source size (see Fluke and Webster 1999 for curvature allowance). The caustic must be isolated lest the source cover several caustics simultaneously. In addition, it is implied that there is no large-scale time gradient in amplification variations. Thus, for example, introducing a constant slope as an additional free parameter allows a model curve of image C to be easily fitted to the entire observing period 1997–1999. However, since there were no such large gradients throughout the entire 15-year-long monitoring history of Q2237+0305 and since their physical origin is not completely understood, we have to abandon the additional parameter.

Finally, the problem can be further complicated by intrinsic quasar variability. In general, the latter is rather difficult to separate from microlensing variability. However, given that the delays between the images in our cases do not exceed several days, intrinsic quasar variability must be repeated in all quasar images (with individual amplification factors) virtually simultaneously. The fact that the brightness variations in all four components are not synchronous provides circumstantial evidence that intrinsic quasar variability is negligible in this source.

Despite the possible complicating factors listed above, we have every reason to believe that the simple model used here is capable of faithfully reproducing the observational data, and that its implications deserve a careful analysis.

After this paper was mainly complete, Wyithe et al. 2000 independently published a preprint where they also interpreted the OGLE-group observations of Q2237+0305. These authors analyzed the light curves by using statistical methods based on conditional probability distributions.

Wyithe et al. 2000 focused mainly on computing the probability of occurrence of brightness bursts with observed parameters and on estimating the possibility of subsequent bursts. The conclusion that there is an additional overlooked brightness burst in image C associated with caustic crossing between the observing seasons of 1997 and 1998 seems of considerable interest. Such an event can account for the difficulties of modeling the light curve for image C in terms of the model with a single caustic crossing. Wyithe et al. 2000 also expect another caustic crossing in image C 500 days after the 1999 summer maximum (with a large uncertainty of $\sim 100 - 2000$ days, though).

The amplification in image A in late 1999 is interpreted as caustic crossing in the negative direction, just as we did here. However, the peak of image C in mid-1999 is assumed to be caused by the passage of the source near the caustic cusp. The choice between the two interpretations of image C variability could be made by analyzing color variations of the source, which are much larger during caustic crossing than during cusp passage. A color analysis could be performed by invoking additional data of the simultaneous monitorings at the Apache Point and Maidanak Observatories (Bliokh et al. 1999) through various filters during the same observing period.

Acknowledgments. I wish to thank the OGLE group for organizing and carrying out the monitoring of Q2237+0305 and for providing access to the data before their publication.

REFERENCES

- Agol E. and Krolik J., *Astrophys. J.* **524**, 49 (1999)
 Blandford R. D. and Narayan R., *Astrophys. J.* **310**, 568 (1986)
 Bliokh P. V., Dudinov V. N., Vakulik V. G. et al., *Kinematika Fiz. Nebesnykh Tel* **15**, 338 (1999)
 Chang K. and Refsdal S., *Astron. Astrophys.* **132**, 168 (1984)
 Corrigan R. T., Irwin M. J., Arnaud J. et al., *Astron. J.* **102**, 34 (1991)
 Fluke C. J. and Webster R. L., *Mon. Not. Roy. Astron. Soc.* **302**, 68 (1999)
 Grieger B., Kayser R., and Schramm T., *Astron. Astrophys.* **252**, 508 (1991)
 Irwin M. J., Webster R. L., Hewett P. C. et al., *Astron. J.* **98**, 1989 (1989)
 Lewis G. F. and Irwin M. J., *Mon. Not. Roy. Astron. Soc.* **283**, 225 (1996)
 Manmoto T., Mineshige S., and Kusunose M., *Astrophys. J.* **489**, 791 (1997)
 Mineshige S. and Yonehara A., *Publ. Astron. Soc. Jpn.* **51**, 497 (1999)
 Østensen R., Refsdal S., Stabell R. et al., *Astron. Astrophys.* **309**, 59 (1996)
 Press W, Teukolsky S., Vetterling W. et al. *Numerical Recipes in FORTRAN* (Cambridge Univ. Press, Cambridge, 1992, 2nd ed.), p. 675
 Schneider P. and Wagoner R. V., *Astrophys. J.* **314**, 154 (1987)
 Schneider P. and Weiss A., *Astron. Astrophys.* **171**, 49 (1987)
 Shakura N. I. and Sunyaev R. A., *Astron. Astrophys.* **24**, 337 (1973)
 Wambsganss J., Witt H. J., and Schneider P., *Astron. Astrophys.* **258**, 591 (1992)
 Wozniak P. R., Alard C., Udalski A. et al., *Astrophys. J.* **529**, 88 (2000)
 Wyithe J. S. B., Webster R. L., and Turner E. L. , *Mon. Not. Roy. Astron. Soc.* **309**, 261 (1999)
 Wyithe J. S. B., Turner E. L., and Webster R. L. , *astro-ph/0001307* (2000)
 Zakharov A. F., *Gravitational Lenses and Microlenses* (Yanus, Moscow, 1997)
 Zakharov A. F. and Sazhin M. V., *Usp. Fiz. Nauk* **168**, 1041 (1998) (*Phys. Usp.* **41**, 945 (1998))